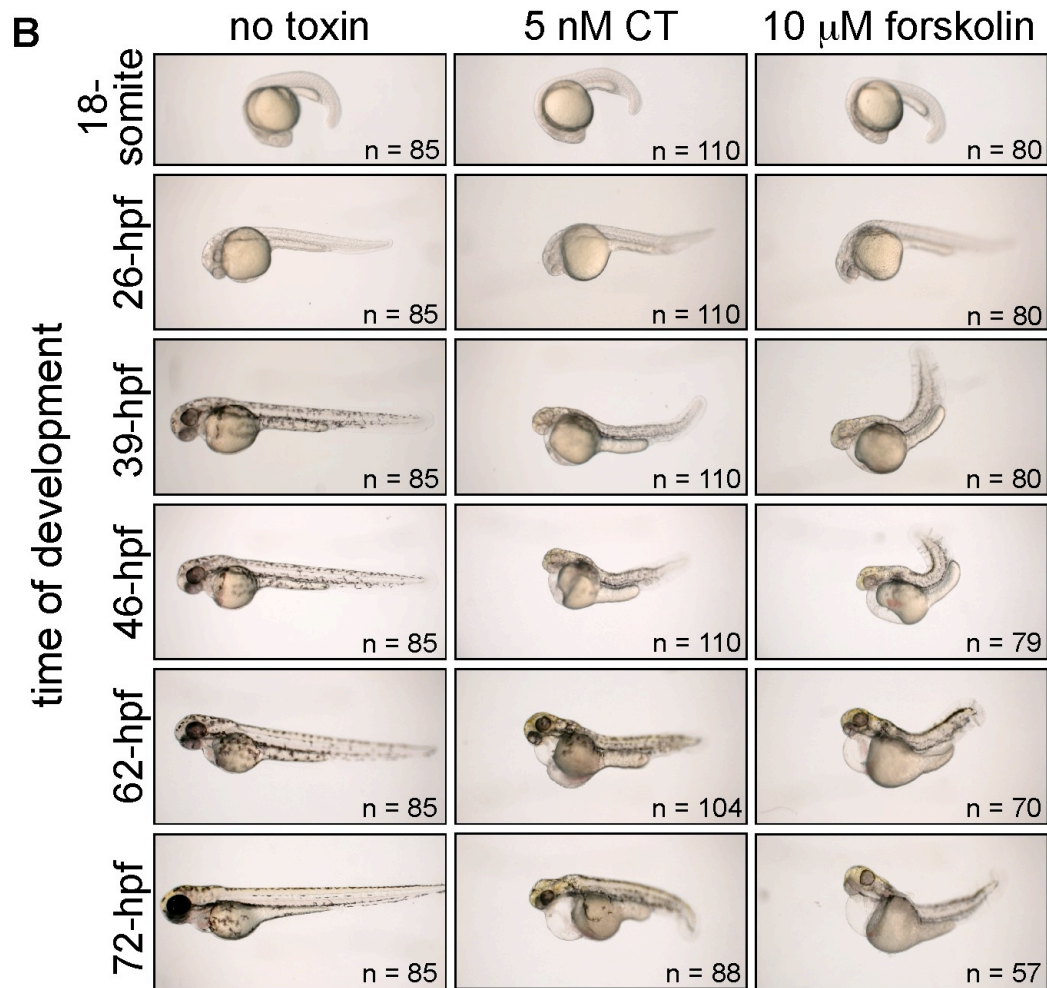
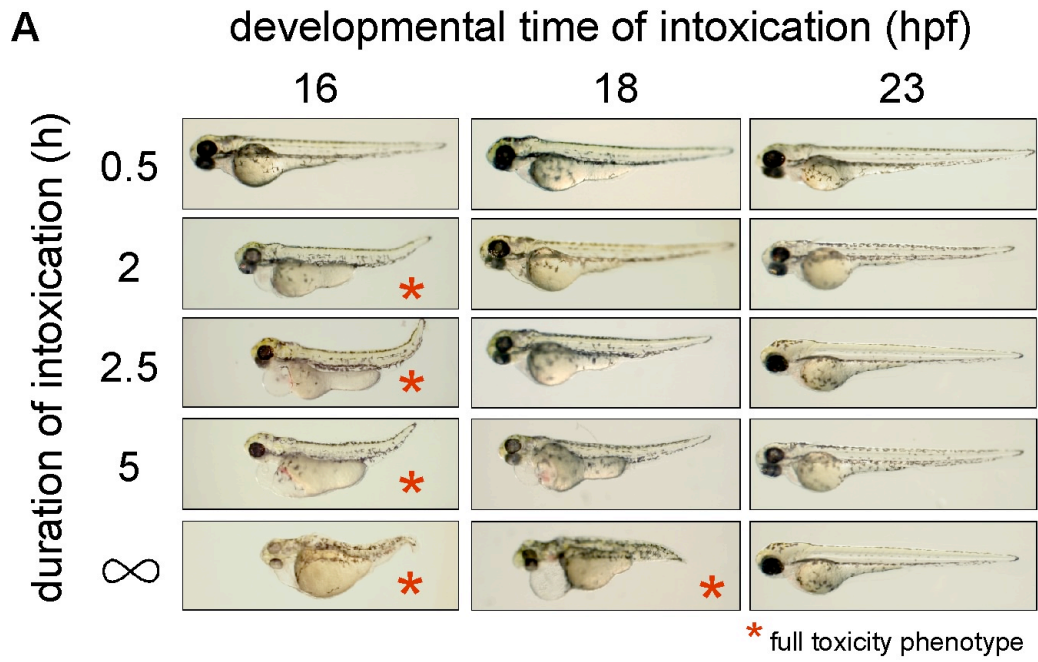
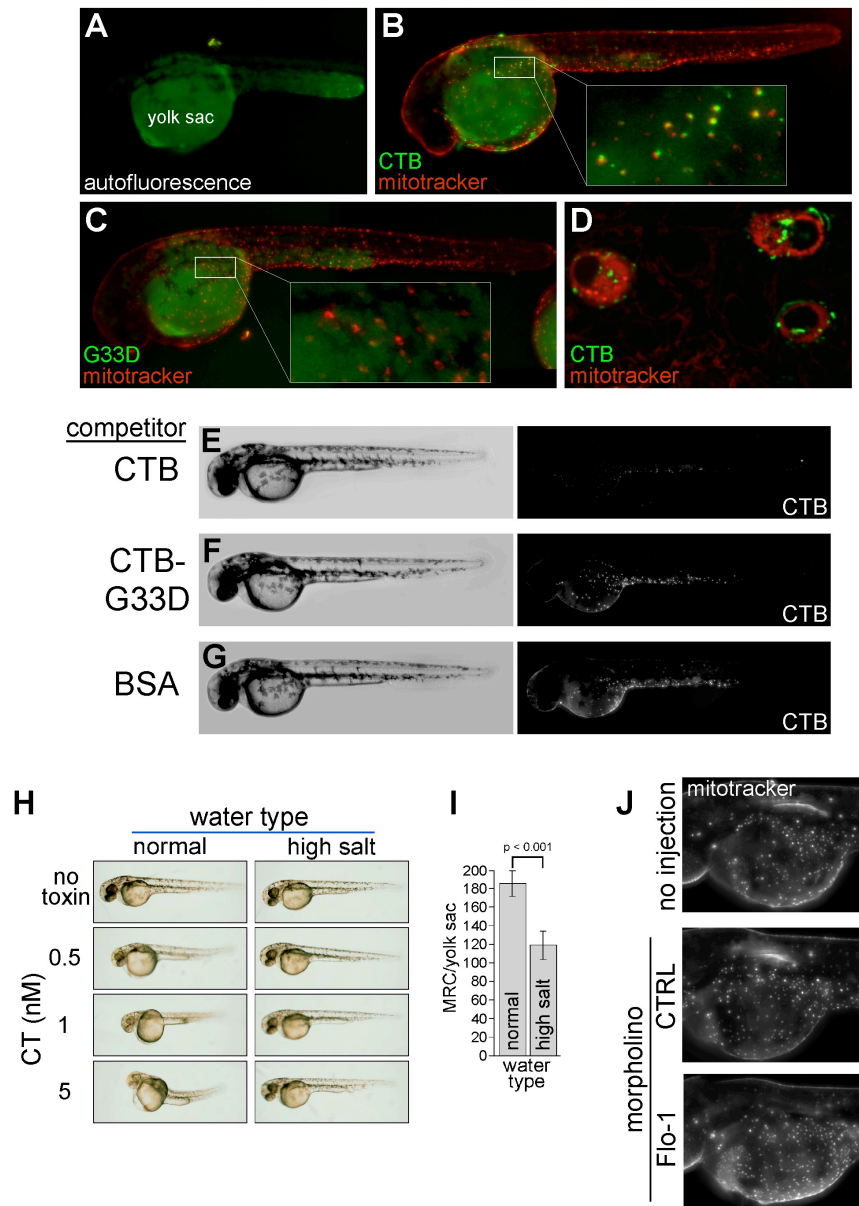


SUPPLEMENTAL DATA



Supplemental Figure 1. Intoxication depends on stage of embryo development, duration of exposure, and displays an early time-course of action.

(A) 5 nM CT was applied to all embryos at the indicated developmental periods (columns) for the indicated durations (rows; bottom is continuous intoxication), and imaged at 72-hpf. Asterisk indicates full toxicity; $n \geq 45$ for each time point and full experiment was performed twice (16-hpf intoxication stage was performed four times). (B) 18-somite stage Tü embryos were treated as indicated. Representative embryos were followed and imaged at the time of development indicated at left. Note: decreasing n is due to embryo mortality.



Supplemental Figure 2. CTB binding and internalization into mitochondrion-rich epithelial cells (MRCs).

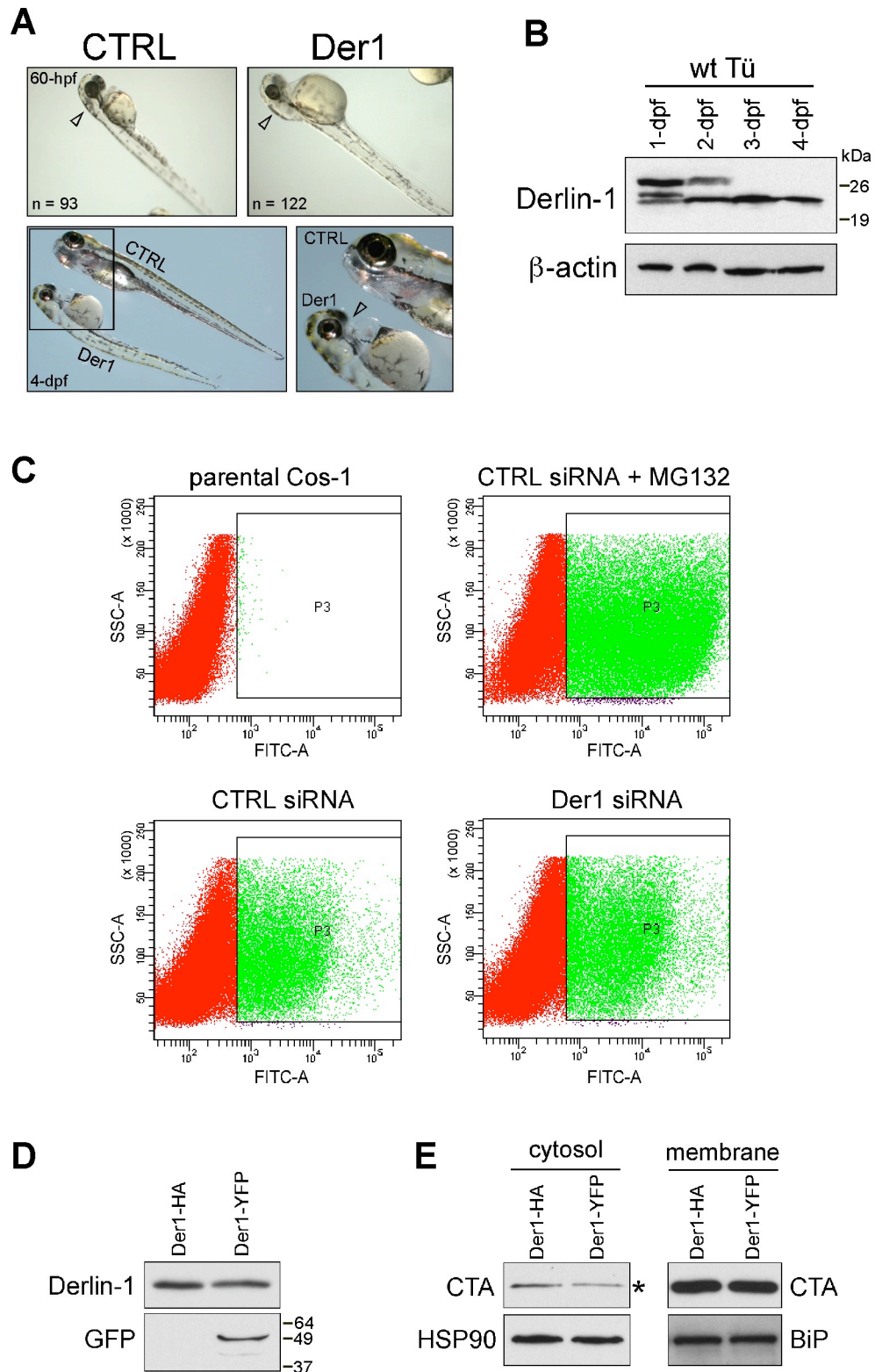
To determine which cell type(s) in the zebrafish embryo were binding and internalizing CT, we incubated 10 40-hpf embryos for 1 h with fluorescently-labeled WT or mutant G33D CTB (20 nM). Fluorescence microscopy was then performed in 3-dimensions on live, anesthetized embryos, and images portrayed as collapsed stacks of individual optical sections. Control embryos exposed only to embryo water exhibited diffuse autofluorescence emanating largely from the yolk sac (**A**). Embryos exposed to WT CTB displayed dense, punctate labeling scattered over the surface of the yolk sac (**B**), whereas no signal was detectable in embryos exposed to fluorescent CTB-G33D (**C**). Small boxes indicate the region of the enlarged inset in **B** and **C**. The CTB signal was abolished by competition with unlabeled WT CTB (**E**, right panel), but not with CTB-G33D or BSA (**F** and **G** respectively, right panels), showing specificity for GM1 binding (and GM1-mediated endocytosis; see below). Rapid movement of WT CTB through the endosomal network on vesicles and extended tubules was observed by confocal microscopy at higher magnification in live

embryos (**D** and see Supplemental Movie 1), indicating that the puncta in **B** are epithelial cells that have internalized CTB.

The labeling observed for CTB was coincident with cells that labeled strongly with either the mitochondria-specific marker MitoTracker (**B**), or ConA (data not shown). These criteria identify the cell types internalizing the toxin as mitochondrion-rich cells (MRC) and proton-secreting cells, respectively; both operate cooperatively in the zebrafish embryo to regulate salt and water homeostasis (34).

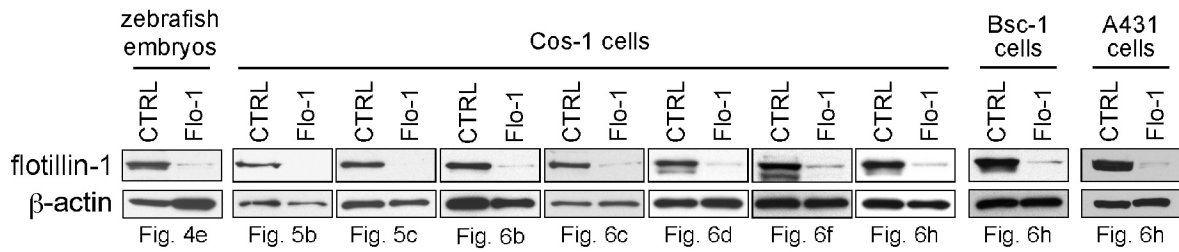
We also tested if CT might induce toxicity in zebrafish by acting on MRCs. Previous studies show that zebrafish embryos adapt to brackish (high salt) water by down-regulating MRC cell numbers, thus altering salt and water transport function (34). As such, embryos were hatched and raised in normal embryo water or in water with elevated salt content (see Methods). At 16-18-hpf, embryos were exposed to varying concentrations of CT or kept in the same embryo water as controls (no toxin). All embryos (>50 embryos/condition) grew and developed normally to 48-hpf by accommodating to salt content as expected (**H**, no toxin), however, embryos raised in high salinity exhibited complete resistance to CT and possessed fewer MRCs as compared to controls (**H** and **I**). Thus, alteration in MRC cell number, and presumably MRC physiology, correlated with sensitivity to intoxication by CT suggesting that CT induces toxicity in zebrafish by invading this cell type. (**I**) MRCs were quantified (stained and imaged as above) from six embryos reared in the indicated water type. Data are mean \pm s.d.

Studies on embryos depleted of flotillin-1/-2 (reggie-2/-1): (**J**) 48-hpf uninjected, control, and flotillin-1 morphants were incubated for 10 min with MitoTracker and imaged as above. No gross differences were observed in overall MRC cell number in the 10 embryos imaged/condition. Similar results were obtained at 3-dpf (data not shown).



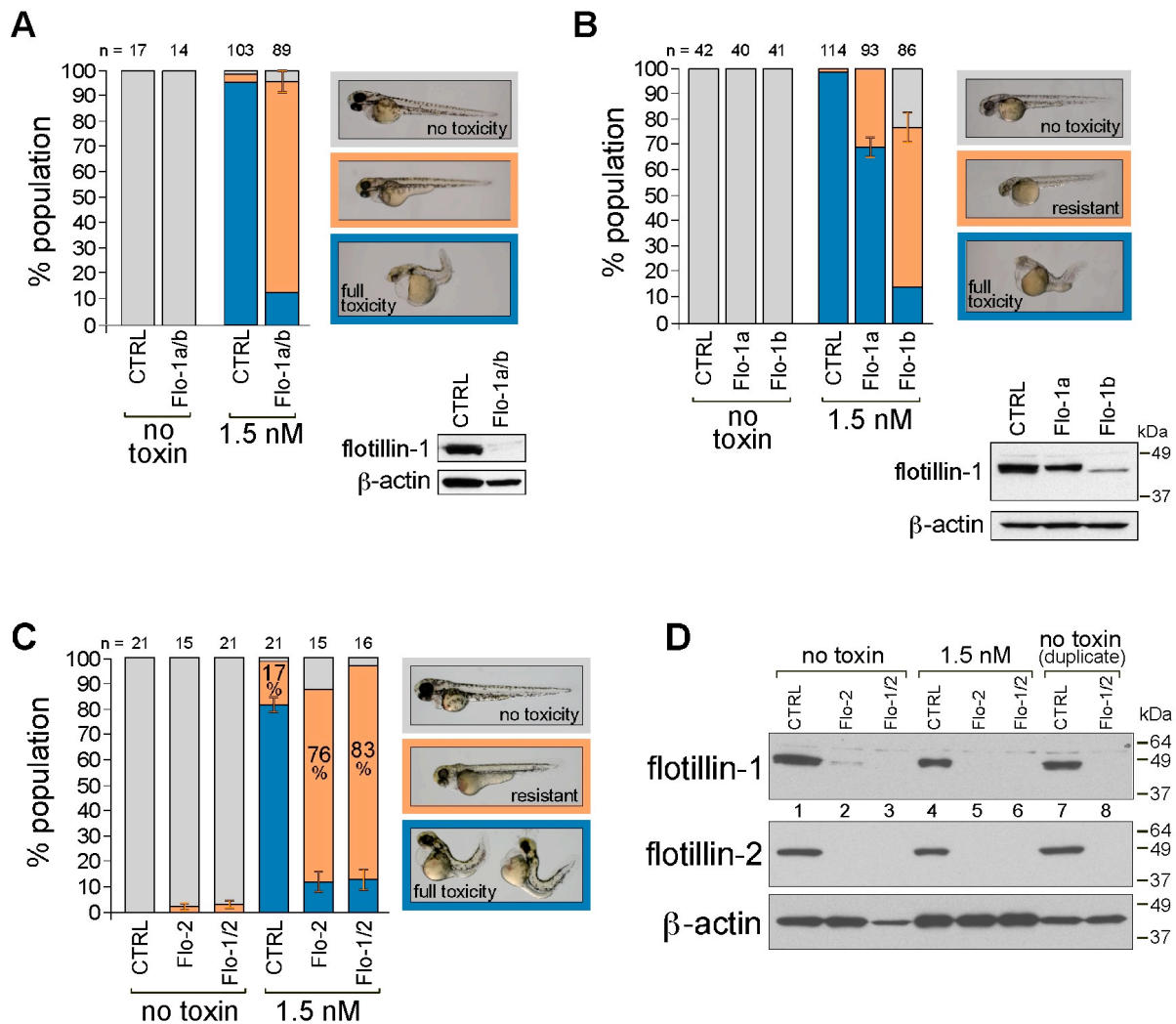
Supplemental Figure 3. Further investigations of Derlin-1 in zebrafish embryos and mammalian cells.
(A) Unintoxicated control and Derlin-1 morphants were imaged at 60-hpf (upper panels) and 4-dpf (lower panels). Boxed area is shown at higher magnification in bottom right panel. Arrowheads indicate altered head and jaw morphologies in Derlin-1 morphants. **(B)**

Immunoblot analysis of Derlin-1 content in crude protein extracts from 1-, 2-, 3-, and 4-dpf Tü embryos (pools of 15 individuals/sample). The slower migrating bands present in the 1- and 2-dpf samples that label with Derlin-1 Ab are likely authentic Derlin-1 that has been shifted, possibly due to the higher proportion of yolk lipids to extracted proteins in less developed embryos (notice slower migration of β -actin in these two samples as well). **(C)** Representative raw flow cytometry data with indicated gate (P3) for the experiments shown in Figure 3F. **(D)** Cell lysates of Cos-1 cells transfected for 48 h with 2 μ g Derlin-1-HA or Derlin-1-YFP DNA using Lipofectamine were analyzed by immunoblot using Derlin-1 and GFP antibodies (~80% of cells were transfected as gauged by YFP fluorescence). MW standards are indicated. **(E)** Dominant-negative Derlin-1 reduces CT A1-chain retro-translocation after 45 min of intoxication. A1-chain retro-translocation was measured as in Figure 3D. Asterisk denotes slightly decreased (~30%) A1-chain present in the cytosolic fraction from intoxicated cells expressing the dominant-negative Derlin-1-YFP as compared to Derlin-1-HA control.



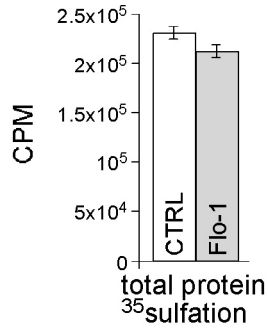
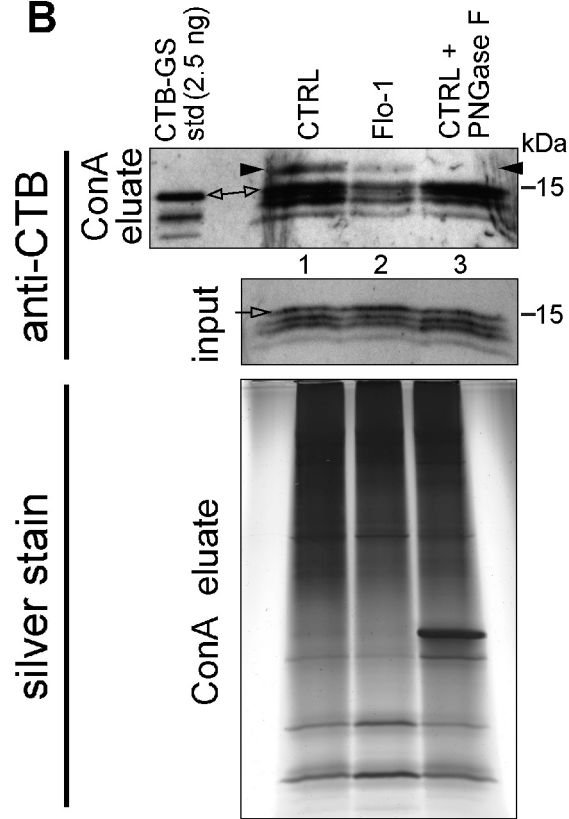
Supplemental Figure 4. Immunoblot analysis of flotillin-1 after depletion by morpholino and siRNA.

For each indicated experiment, crude protein extracts prepared either from pools of 5, 68-72-hpf control or reggie-2/flotillin-1 morphants or 5×10^5 mammalian cells transfected with control or flotillin-1 siRNA were immunoblotted for flotillin-1 as in Figure 4A and Figure 5A.



Supplemental Figure 5. Loss of flotillin-1b (reggie-2b) confers a higher degree of CT resistance than flotillin-1a (reggie-2a) and depletion of both flotillin-1 and -2 (reggie-2 and -1) confers similar resistance to CT as flotillin-1 alone.

(A) Embryos injected with either control or a combination of flotillin-1a and -1b morpholinos were intoxicated with 1.5 nM CT or embryo water only (no toxin) and scored for phenotype as in Figure 4B and C. Results are representative of two independent experiments. Total protein was extracted from unintoxicated pools of 5, 72-hpf embryos and analyzed by immunoblot using flotillin-1 and β -actin (bottom right). (B) Embryos injected with control, flotillin-1a, or flotillin-1b morpholinos were intoxicated with 1.5 nM CT or embryo water only (no toxin) and scored for phenotype as in panel A. Results are representative of three independent experiments. Total protein was extracted from unintoxicated pools of 5, 72-hpf embryos and analyzed as in A (bottom right). (C) Embryos injected with control, flotillin-2, or a combination of flotillin-1 (targeting both homologs) and -2 morpholinos were intoxicated with 1.5 nM CT or embryo water only (no toxin). Morphants were binned into one of three phenotype categories (right panels) and results summarized as in Figure 4C. (D) Total protein was extracted from pools of 5 72-hpf embryos and analyzed by immunoblot using flotillin-1 and -2 antibodies and β -actin for protein equivalency.

A**B**

Supplemental Figure 6. Additional controls for sulfation-glycosylation assay for CTB transport into the TGN and ER.

(A) Total protein from the Cos-1 cell lysates in experiment Figure 6C were precipitated by TCA and radioactivity assessed by scintillation counts as previously described (63); reported as counts per minute (CPM). (B) An independent replicate of the experiment shown in Figures 6D and 6E with the addition of treatment of a fraction of the control sample with PNGase F to demonstrate N-glycosylation (lane 3, arrowhead). Additionally, a fraction of the cell lysate from each sample was immunoblotted for CTB (input). Arrows indicate full-length CTB-GS.

Supplemental Movie 1. Intracellular movement of labeled CTB (green channel) in MRC cells (labeled with MitoTracker in red channel) from live, anesthetized 40-hpf embryos as shown in Supplemental Figure 2B and 2D. Time-lapse sequence over 100 s.

Supplemental Movie 2. Dynamics and localization of flotillin-1-GFP and fluorophore-labeled CTB in live Cos-1 cells.

Control or flotillin-1-depleted cells were transiently transfected with flotillin-1-EGFP (for 16 h) and were pulsed with 20 nM CTB-alexa 594 nm for 1 h at 37°C. Low GFP-expressing cells were chosen for live-cell imaging. Left panel is flotillin-1-GFP, middle panel, CTB, and right panel, merged image. Confocal sections were captured every 0.5 s, for a total time-lapse of 100 s. Note co-localization of CTB and flotillin-1-GFP at the PM and in endosomal compartments.

Supplemental Movie 3. Control or flotillin-1-depleted Cos-1 cells were incubated with fluorophore-labeled CTB for 120 min and immunostained for PDI. Arrowheads indicate outline of NE. Note the absence of CTB NE signal in flotillin-1-depleted cells (control cell scored positive in assay, flotillin-1-depleted cell scored negative). Movie toggles between CTB only and CTB/PDI merged images (use keyboard arrows to slowly turn on/off channel representing PDI). Scale bar = 10 μ m.

Supplemental References

63. Sandvig, K., Garred, Ø., Prydz, K., Kozlov, J.V., Hansen, S.H., and van Deurs, B. 1992. Retrograde transport of endocytosed Shiga toxin to the endoplasmic reticulum. *Nature (Lond.)* 358:510-511.